LEVEL

EROSIVE BURNING OF COMPOSITE SOLID PROPELLANTS: EXPERIMENTAL AND MODELING STUDIES

Merrill K. King

August, 1978

ATLANTIC RESEARCH CORPORATION
Research and Technology Division
5390 Cherokee Avenue
Alexandria, Virginia 22314

Contract F49620-78-C-0016

Air Force Office of Scientific Research
Building 410
Bolling AFB, D.C. 20332

EROSIVE BURNING OF COMPOSITE SOLID PROPELLANTS: EXPERIMENTAL AND MODELING STUDIES*

Dr. Merrill K. King**
Atlantic Research Corporation
Alexandria, Virginia 22314

Abstract

An experimental apparatus designed for measurement of erosive burning rates at crossflow velocities up to Mach 1 has been used to determine the erosive burning characteristics of seven propellant formulations with systematically varied properties. A composite propellant erosive burning model based on the bending of columnar diffusion flames gives reasonably good agreement with the measured erosive burning data over a wide range of conditions, breaking down only in regions where the fuel-oxidizer gas stream mixing does not control burning rate. Propellant base (no-crossflow) burning rate is found to have a predominant effect on sensitivity to crossflow (higher-burning-rate formulations being considerably less sensitive) whether the base burning rate differences are produced by oxidizer particle size variation, oxidizer/fuel ratio variation, or use of catalysts. Comparison of erosive burning predictions using the erosive burning model described herein with flow profiles expected to prevail in the test apparatus to predictions using profiles believed to exist in cylindrically-perforated motor grains indicate that erosive burning may be considerably less for a given mainstream crossflow velocity in such a motor than in the typical erosive burning test apparatus, a result quite important to extrapolation of test apparatus erosive burning data to actual motor conditions.

Introduction and Background

Erosive burning, the augmentation of solid propellant burning rate by the flow of products across a burning surface, is becoming increasingly important with use of lower port-to-throat area ratio motors and nozzleless motors both of which result in high velocity crossflows. The response of various propellants to such crossflows must be known by the motor designer in order for him to perform adequate motor design. In addition, it is important that the propellant formulator understand the effect of various formulation parameters on the sensitivity of a propellant to crossflows so that he may tailor his propellants to the desired characteristics. For example, in a nozzleless rocket motor, the decrease in pressure from the head end to the aft end of the grain tends to result in slower burning at the aft end in the absence of erosive effects. Depending upon the sensitivity of the formulation to crossflow, the increasing Mach Number along the grain port may lead to undercompensation, exact cancellation, or overcompensation of the pressure effect. (The effects of erosive burning on solid propellant rocket interior ballistics for low port-to-throat area ratio motors and nozzleless motors are discussed further in Reference 1.)

General observations of importance from the past experimental studies[2-11] include:

1. Plots of burning rate versus gas velocity or mass flux at constant pressure are usually not fitted best by a straight line.
2. Threshold velocities and "negative" erosion rates are often observed.
3. Slower burning propellants are more strongly affected by crossflows than higher burning-rate formulations.
4. At high pressure and crossflow velocity, the burning rate under erosive conditions tends to approach the same value for all propellants (at the same flow velocity) regardless of the burning rate of the propellants at zero crossflow.
5. Erosive burning rates do not depend upon gas temperature of the crossflow (determined from tests in which various "driver propellant's" products are flowed across a given test propellant).

There is, however, very little data available for high crossflow velocities (greater than $M \approx 0.3$). In addition, there has been no erosive burning study in which various propellant parameters have been systematically varied one at a time. Such a study is necessary for elucidation of erosive burning mechanisms and proper modeling of the erosive burning phenomena. Much of the past work has not resulted in instantaneous (as opposed to averaged over a range of pressure and crossflow velocity) measurements of erosive burning rates under well-characterized local flow conditions.

Over the years, a large number of models of erosive burning of composite (heterogeneous) and double-base (homogeneous) propellants have been developed: most of these models have been reviewed by this author in References 1, 12, and 13. Of the models other than the one developed by this author[12,13] those of Lengelle,[14] Beddini, et al[15,16,17] Razdan and Kuo[18], and Osborn, et al[19] appear to be the most advanced. Common to all four of these models is the assumption that the increase in propellant burning rate associated with crossflow results from turbulence generated by this crossflow penetrating between the propellant gas flame zone(s) and the surface, causing increases in mass and energy transport rates.

Application of an energy balance at the surface of a burning propellant, with the heat flux from gas-phase driving reactions equated to the product of propellant mass burning flux and the net energy per unit mass required to heat the ingredients to the surface temperature and vaporize/decompose them (even allowing for considerable exothermic surface decomposition as in the Beckstead-Derr-Price[20]

* Research sponsored by the Air Force Office of Scientific Research (AFSC), United States Air Force, under Contracts F44620-76-C-0023 and F49620-78-C-0016. The United States Government is authorized to reproduce and distribute reprints for governmental purposes notwithstanding any copyright notation hereon.

** Chief Scientist, Research and Technology, Member AIAA.

model) indicates that the burn-rate-controlling gas-phase heat release must occur within 5 to 20 microns of the propellant surface for typical burning rates of 1 to 4 cm/sec. (These "effective flame-height" numbers were calculated from intermediate output of a fundamental composite propellant combustion model being developed by this author[21]: their validity is supported by the fact that this model yields predicted burning-rate versus pressure curves in good agreement with data for unimodal oxidizer composite propellants containing oxidizer ranging from 5 to 200 microns in diameter.)

On the other hand, use of the universal u^+, y^+ flow profile correlation (transpiration effects neglected), with the edge of the laminar sublayer being defined by $y^+=5$, indicates laminar sublayer thicknesses of 32, 14, and 8 microns for crossflow velocities of 60, 150, and 300 m/sec (200, 500, and 1000 ft/sec) at a pressure of 5 MPa (50 atmospheres), this thickness increasing with decreasing pressure. Moreover, data of Mickley and Davis[22] indicate that this sublayer thickness is increased by transpiration (in our case, evolution of oxidizer and binder decomposition products from the propellant surface). For example, for a ratio of transpiration flow to cross flow of 0.01 (the upper limit of their study) their measurements indicate that the laminar sublayer thicknesses for the three crossflow velocities listed above will increase to 140, 60, and 30 microns, respectively. (It should be pointed out, though, that their measurements indicate zero-transpiration sublayer thicknesses of 85, 35, and 20 microns at these crossflow velocities, corresponding to a critical y^+ of 13 instead of 5.) These calculations indicate to this author that it is quite possible that crossflow-induced turbulence does not penetrate into the region between the driving gas-phase heat release and the surface (though the evidence does not appear to be conclusive).

In addition, even if the turbulent region does extend into this zone, in order for the eddies to have significant effect on mixing and thus on heat and mass transfer, they must be considerably smaller than the flame offset distance; that is, they must be on the order of one micron in diameter or less. It is not clear to this author that a significant amount of turbulence of this scale will be induced in the zone between the propellant surface and the gas-phase flame zone(s) by crossflow. Accordingly, an alternate possible mechanism for erosive burning of composite propellants, not dependent on the augmentation of transport properties in the combustion zone by crossflow-induced turbulence, is postulated. This mechanism, involving the bending over of columnar diffusion flames by a crossflow (discussed briefly below) has been incorporated into a "first generation" model described in detail in References 12 and 13, and is currently being incorporated into a more fundamental "second generation" model.[21]

Flame-Bending Erosive Burning Model Description

In the combustion of composite solid propellants, it is generally accepted that parallel columns of oxidizer and binder sublimation/decomposition product gases leave the surface from above the oxidizer crystals and binder, respectively. In the most general case some heat is fed back to the surface from monopropellant reaction of oxidizer sublimation products while additional heat is supplied by the mixing and reaction of the oxidizer and fuel product streams. Accordingly, an important factor in determining the rate of heat feedback (which increases with decreased distance of the gas-phase heat release zone(s) from the surface) is often the rate of mixing of the oxidizer and binder gas product columns. In the absence of a crossflow, these columns move perpendicular to the propellant surface, while, with crossflow, they are tilted over and travel at an angle to the surface, this angle being determined by the ratio of crossflow velocity to transpiration velocity at any given position above the surface. (Since, in general, the crossflow and transpiration velocities will not scale in the same manner with distance from the surface, the flow vector will actually be curved, but in this model it is approximated as a straight line with the angle being determined by the ratio of these two velocities at a distance from the surface corresponding to the end of the mixing region.)

A schematic depicting the first generation composite propellant erosive burning model is presented in Figure 1. In the first part of the figure, we picture the flame processes occurring in the absence of crossflow. There are two flames considered: an ammonium perchlorate deflagration monopropellant flame close to the surface; and a columnar diffusion flame resulting from mixing and combustion of the AP deflagration products and fuel binder pyrolysis products at an average distance somewhat further from the surface. Three important distance parameters considered are the distance from the propellant surface to the "average" location of the kinetically controlled AP monopropellant heat release (L_I), the distance associated with mixing of the oxidizer and fuel for the diffusion flame (L_{Diff}), and the distance associated with the fuel-oxidizer reaction time subsequent to mixing (L_{Kin}). A heat balance (see Reference 13) between heat feedback from these two flames and the energy requirements for heating the propellant from its initial temperature to the burning surface temperature and decomposing it yields (assuming that the heat feedback required per unit mass of propellant consumed is independent of burning rate):

$$r_o \propto q_{feedback} \propto \frac{k_1(T_{AP} - T_s)}{L_I} + \frac{k_2(T_f - T_s)}{L_{Diff} + L_{Kin}} \qquad (1)$$

The situation pictured as prevailing with a crossflow is shown in the second part of Figure 1. Since L_I and L_{Kin} are both kinetically controlled and are thus simply proportional to a characteristic reaction time (which is assumed to be unaffected by the crossflow) multiplied by the propellant gas velocity normal to the surface (which for a given formulation is fixed by burning rate and pressure alone), these distances are fixed for a given formulation at a given burning rate and pressure, independent of the crossflow velocity. (Of course, since crossflow velocity affects burning rate at a given pressure through its influence on the diffusion process as discussed below, L_I and L_{Kin} are influenced through the change in burning rate, but this is simply coupled into a model by expressing L_I and L_{Kin} as explicit functions of burning rate and pressure in that model. The important point is that they can be expressed as functions of these two parameters alone for a given propellant.) However, the distance of the mixing zone from the propellant surface is directly affected by the crossflow. In References 12 and 13, this author simply stated that it could be shown through geometrical arguments coupled with the columnar diffusion flame height analysis presented by Schultz, Penner and

Green[5], that L_{Diff} measured along a vector coincident with the resultant of the crossflow and transpiration velocities should be approximately the same as L_{Diff} normal to the surface in the absence of a crossflow at the same burning rate and pressure (except at very high ratios of local crossflow velocity to transpiration velocity). Personal communications have indicated that it is not obvious how this conclusion was reached without recourse to using augmented transport properties. Accordingly a simplified version of the analysis used in reaching this conclusion is presented in Figure 2, which is essentially self-explanatory. Basically what appears to have worried those questioning the conclusion that the magnitude of L_{Diff} measured in the direction of the flow is independent of that direction is that the time required for a parcel leaving the surface to travel the distance L_{Diff} in the flow direction θ, at constant burning rate, is inversely proportional to the sine of the flow angle. This is indeed true. However, the characteristic mixing time is also decreased since the average concentration gradient is increased by the circular cross-section (in the absence of crossflow) being converted to an elliptical cross-section with major axis d_p and minor axis $d_p \sin\theta$. Obviously, doing an exact calculation of the effect on characteristic mixing time is somewhat difficult: however, replacement of the circle diameter d_p by the geometric mean ellipse diameter $\sqrt{d_p \cdot d_p \sin\theta}$ in calculating concentration gradients does not seem unreasonable. When this is done, the magnitude of L_{Diff}, measured in the flow direction, is calculated to be independent of flow angle, θ, as shown in Figure 2. A somewhat more rigorous (and immensely more complex) analysis has been performed, indicating that the above approximation is quite good for $\theta > 20$ degrees, but that for smaller angles (columns further pushed over) the magnitude of L_{Diff} actually begins to decrease relative to the no-crossflow value.

At any rate, to a reasonably good approximation, the magnitude of L_{Diff} is independent of the crossflow velocity although its orientation is not. Thus, the distance from the surface to the "average" mixed region is decreased to $L_{Diff} \sin\theta$. (See Figure 1.) The heat balance at the propellant surface now yields:

$$r \propto \dot{q}_{feedback} \propto \frac{k_1(T_{AP} - T_s)}{L_I} + \frac{k_2(T_f - T_s)}{L_{Diff} \sin\theta + L_{Kin}} \quad (2)$$

This picture was used as the basis of development of a first generation flame bending model for prediction of burning rate versus pressure curves at various crossflow velocities, given only a curve of burning rate versus pressure in the absence of crossflow. The general approach used in development of this model was:

1. Derive expressions for L_I, L_{Diff}, and L_{Kin} as functions of burning rate (or burning mass flux, $\dot{m}_{burn}$), pressure, and propellant properties and substitute these into a propellant surface heat balance. (Equation 1.)
2. Work the resulting equation into the form:

$$r_o = A_3 P \left[1 + \frac{A_4}{1 + A_5 d_p^2 P^2} \right]^{1/2} \quad (3)$$

for burning in the absence of crossflow and perform a regression analysis using no-crossflow burning rate data to obtain best fit values for A_3, A_4, and A_5. (d_p is the average ammonium perchlorate particle size. For a given propellant, the burning rate data may be just as effectively regressed on A_3, A_4 and $A_5 d_p^2$, eliminating the necessity of actually defining an effective average particle size.)

3. From these results, obtain expressions for L_I, L_{Diff}, and L_{Kin} as functions of burning rate (or $\dot{m}_{burn}$) and pressure.
4. Combine these expressions with an analysis of the boundary layer flow which gives the crossflow velocity as a function of distance from the propellant surface, mainstream velocity, and propellant burning rate, to permit calculation of the angle θ, L_I, L_{Diff}, and L_{Kin}, and $\dot{m}_{burn}$ for a given pressure and crossflow velocity, via Equation 2.

Details of the model development can be found in References 12 and 13. Currently, this same flame-bending mechanism is being built into a more fundamental composite propellant burning rate model for prediction of burning rate versus pressure characteristics with or without crossflow (given only composition and ingredient sizes.)[21]

During the course of this effort, the author became aware of complaints that data on erosive burning taken in test devices where driver grain product gases were passed over small specimens (strips or tablets) of the test propellant did not extrapolate well to motor conditions, the erosive effects being considerably less in actual motors than anticipated from the laboratory results. One possible explanation for this is that the boundary layer flow profiles are considerably different in the test device flow channel than in a motor. In most test devices, including the one used in this program, the ratio of blowing velocity (gas velocity normal to the propellant surface, generated by the combustion) to crossflow velocity is usually quite small (less than 0.02), lying in a range where the data of Mickley and Davis[22] used in the model described above are applicable. Recent work by Yamada, et al.[23] and Dunlap, et al.,[24] however, indicates that in cylindrically perforated motors, where the ratio of blowing velocity to crossflow velocity tends to be much higher (except at the aft end of very long grains), the flow profiles are considerably different, approximating those of an inviscid flow with a no-slip wall boundary condition. In this case, the axial velocity flow profile is given by a cosine law:

$$u_y = \frac{\bar{u}\,\pi}{2} \cos\left\{ \frac{\pi}{2} \left(\frac{(D/2) - y}{D/2} \right)^2 \right\} \quad (4)$$

The model described above was modified to use this profile in place of the one based on Mickley-Davis data described in References 12 and 13. A set of calculations was then run for a motor with a port diameter of 3 cm (1.2 inches) using both types of profiles for comparison. Formulation 4525 (73/27 AP/HTPB, 20 micron diameter AP) was used for these predictions since, as will be shown later, good agreement was found between the Generation 1 Model using the Mickley-Davis profiles and data taken in our test apparatus with this propellant. Results of these calculations are shown in Figure 3. As may be seen, replacement of the Mickley-Davis profiles with the inviscid no-slip profiles results in a considerable reduction in the predicted degree of erosive burning. This is a particularly important

result, pointing out the necessity of correct definition of flow profiles in a given motor configuration for accurate prediction of erosive burning. Thus it appears that further attention need be paid to accurate definition of profiles, not only in cylindrically perforated motors, but in wagon-wheel perforations, star configurations, and any other configurations where it is felt that erosive burning may be important.

Experimental

The experimental test apparatus and procedures employed in this study of erosive burning are described in detail in Reference 12. A schematic of the basic test apparatus is presented as Figure 4. A cylindrically perforated 6C4 driver grain (15.2 cm outside diameter, 10.2 cm inside diameter) whose length is chosen to give the desired operating pressure for a given test, produces a high velocity gas flow through a transition section into a rectangular test section which contains the test grain (generally the same formulation as the driver grain). The contoured transition section is approximately 10 cm (4 inches) long. The test grain extends from the test section back through the transition section to butt against the driver grain in order to eliminate leading edge effects which would be associated with a test grain standing alone. The test grain is approximately 30 cm(12 inches) long (plus the 10 cm extending through the transition section) by 1.90x2.50 cm (3/4 inch and 1 inch) web and burns only on the 1.90 cm face. The flow channel of the test section is initially 1.90 cm x 1.90 cm (3/4 inch x 3/4 inch), opening up to 1.90 cm x 4.45 cm (3/4 inch x 1-3/4 inch) as the test propellant burns back through its 2.54 cm(1 inch) web. For high Mach Number tests, the apparatus is operated in a nozzleless mode with the gases choking at or near the end of the test grain, while for lower Mach Number tests, a 2-dimensional nozzle is installed at the end of the test channel.

During each test, pressure and crossflow velocity varies with time and location along the test grain. (For the nozzleless tests, pressure varies significantly with time and location, while crossflow velocity varies considerably with location but not significantly with time. For tests using a nozzle with an initial port to throat area ratio of 1.5 or higher, on the other hand, pressure does not vary strongly with location but does rise with time due to the progressivity of the driver grain, while crossflow velocity varies strongly with time and slightly with location.) These variations permitted design of tests to yield considerable burning rate-pressure-crossflow velocity data in relatively few tests, provided that these parameters could be measured continuously at several locations along the test grain. These parameters were measured in the following manner.

The burning rate was directly measured by photographing the ablating grain with a high-speed motion picture camera through a series of four quartz windows located along the length of the test section. Frame by frame analysis of the films allowed determination of instantaneous burning rate as a function of time at each of the four window locations.

For nozzled cases, the measured location of the burning propellant surface at each window as a function of time, together with the known constant throat area, permitted straightforward calculation of the crossflow velocity as a function of time. However, the very sensitive dependence of Mach Number on area ratio for $M > 0.5$ made calculation of crossflow velocity from area ratio measurement quite poor for nozzleless cases. Accordingly, for these tests, stagnation pressure was determined at the aft end of the test section and used in combination with the driver chamber pressure for calculation of the stagnation pressure in the test section as a function of time and position. (Static pressure wall taps at each window location were used for measurement of static pressure as a function of time for both nozzled and nozzleless cases.) From the static and stagnation pressure values determined as a function of time and position down the test section, crossflow Mach Number and velocity were calculated as a function of time at each window location in the test section for the nozzleless cases.

The rationale of the experimental part of this program was to measure the erosive burning characteristics, over a wide range of pressure and crossflow velocity, of a series of propellants in which various formulation parameters were systematically varied. To date, seven formulations, listed in Table I have been studied. The first five of these are "scholastic" formulations. (These are referred to as "scholastic" formulations in that they are formulations specifically chosen to permit systematic variation of well-defined composition and ingredient-size parameters, including the use of unimodal ammonium perchlorate particle size, but as a consequence are not formulations being currently considered for mission applications.) It was considered that the use of unimodal oxidizer in early testing was important, since any model permitting prediction of burning rate-pressure-crossflow velocity characteristics from first principles will almost certainly be first perfected for unimodal oxidizer. (Methods

Table 1. Formulations Tested to Date

Number	Composition	Rationale
1(4525)	73/27 AP/HTPB, 20μ AP	Baseline Formulation, T = 1667°K
2(5051)	73/27 AP/HTPB, 200μ AP	Compare with 1 for AP Size Effect
3(4685)	73/27 AP/HTPB, 5μ AP	Compare with 1 and 2 for AP Size Effect
4(4869)	72/26/2 AP/HTPB/Fe_2O_3, 20 μ AP	Compare with 1 for BR Effect at Constant AP Size
5(5542)	77/23 AP/HTPB, 20μ AP	Compare with 1 for Mix Ratio (Temperature) Effect at Constant AP Size. T = 2065°K
7(5565T)	82/18 AP/HTPB, Bimodal AP (68.35% 20μ, 13.65% 90μ)	Medium Temperature HTPB Formulation. AP Sizes Chosen to Match BR of No. 1, Compare with 1 for Temperature Effect. T = 2575°K.
8(5555T)	82/18 AP/HTPB, Bimodal AP (41% 1μ, 41% 7μ)	Compare with 7 for BR Effect. T = 2575°K.

of handling multimodal oxidizer sizes for predictions of burning rates even in the absence of crossflows are still the subject of considerable debate.) Formulation 1 (also referred to as Formulation 4525) is a baseline 1667°K HTPB formulation (73/27 AP/HTPB) for the initial test series. Formulations 2, 3, and 4 (5051, 4685 and 4869) were selected for investigation of the interrelated effects of oxidizer particle size and base (no crossflow) burning rate. Formulations 1 and 4 are essentially identical except for use of burning rate catalyst to change base burning rate. Formulations 2 and 3 differ from Formulation 1 in oxidizer particle size (200, 5 and 20 micron AP, respectively), and as a consequence, also in base burning rate. Comparison of results from tests with these four formulations permits isolation of the oxidizer particle size and base burning rate effects on sensitivity of propellant burning rate to crossflow.

In terms of independent veriables, Formulation 5 (5542T) differs from Formulation 1 only in terms of oxidizer/fuel ratio (77/23 versus 73/27, yielding a higher flame temperature (2065°K vs. 1667°K) and a different burning rate, oxidizer size being held constant. Thus comparison of the results for these formulations permits definition of the effect of oxidizer/fuel ratio change at constant oxidizer particle size. With Formulation 7 (5565T), on the other hand, oxidizer/fuel ratio is varied from that of Formulation 1 (82/18 vs. 73/27), but oxidizer sizes are changed to give approximately the same zero-crossflow burning rate-pressure curve for the two formulations - this permits examination of the effect of varying oxidizer/fuel (and thus flame temperature) at constant base burning rate. Formulation 8 (5555T) is identical to Formulation 7 except for use of much finer oxidizer to yield higher base burning rate.

A total of 45 tests have been carried out with these seven formulations. Of these, 39 yielded useful data, while six were failures due to breakup of the test grain (in nozzleless tests) or due to camera failure. The rationale and ballistics analyses used in selecting specific test conditions employed were discussed in detail in Reference 12. Basically, the first three tests were designed to yield erosive burning data for Formulation 1 over a range of crossflow velocities of 180 to 350 m/sec (600 to 1200 ft/sec) and a range of pressures of 1.4 to 8.2 MPa (200 to 1200 psia). The next three tests were chosen to examine the same formulation over a crossflow velocity range of approximately 600 to 850 m/sec (2000 to 2800 ft/sec) and a pressure range of 1 to 5 MPa (150 to 750 psia). Tests 7 and 8 differed from Tests 1 and 3 only in having no test grain in the transition section. These tests were aimed at determining the sensitivity of erosive burning to major upstream geometry changes. Tests 9 and 10 differed from Tests 1 and 3 only in their use of a hotter (2400°K) driver formulation with the baseline test formulation (1667°K flame temperature). The purpose of these tests was to determine whether the "core" crossflow gas temperature affected the erosive burning of a given formulation. Tests 11-15, 16-20, 21-25, 26-30, 31-35 and 36-40 were designed to be analogous to Test 1-5 with replacement of Formulation 1 (4525) by Formulations 2, 3, 4, 5, 7 and 8 (5051, 4685, 4869, 5542T, 5565T, and 5555T). Tests 41-45 were added to fill in data gaps revealed by earlier tests.

Results of the tests made for study of the effect of upstream flow conditions (two tests conducted at essentially identical conditions to tests in the main test series, except for the absence of test grain in the transition section) are presented in Figures 5 and 6. As may be seen, the effects of the upstream flow change were quite small, the differences in burning rate augmentation ratio between corresponding tests varying essentially only to the degree predicted by the slight difference in pressure-crossflow velocity-time history in the matched tests. Accordingly, it is concluded that the erosive burning measured at the viewing ports is not particularly sensitive to the driver grain-transition section contours in the test apparatus. This result is consistent with an observation that the augmentation rates do not vary significantly with window location for the nozzled tests (where pressure and crossflow velocity are nearly the same at each window location at any given time).

As discussed in References 1, 12, and 13, erosive burning models based on increased heat transfer from a "core" gas flow (notably the widely used model of Lenoir and Robillard[25]), predict that with a given test section propellant, variation of the flame temperature of the driver propellant should lead to variation in the erosive burning augmentation ratio at fixed crossflow velocity and pressure. Two pairs of tests (1 and 9, 3 and 10), in which the driver grain flame temperature was varied from 1667°K to 2425°K, while the test section propellant was held constant and crossflow velocity and pressure versus time histories were held as nearly constant as possible, were carried out in this study. Results are presented in Figures 7 and 8. In each figure, measured burning rate augmentation-ratio and the ratio predicted using the first generation model described earlier are plotted against time for each of the paired tests. (The predicted values are presented to permit a zeroing out of the slight differences in pressure and crossflow velocity versus time histories of the paired tests. The different "core" gas temperatures in the paired tests are seen to have negligible effect on the erosive burning characteristics of the test propellant.

A rather complete set of data, covering a pressure range of 1 to 5 MPa (10 to 50 atmospheres) and a crossflow velocity range of 180 to 670 m/sec (600 to 2200 ft/sec) has been obtained for Formulation 4525, the baseline formulation. Experimental results and theoretical predictions (based on the model described earlier) are presented in Figures 9 and 10. As may be seen, agreement between predictions and data is reasonably good. The predicted curves for burning rate versus pressure at various crossflow velocities (Figure 9) do seem to group more tightly than the data. That is, as shown more clearly in Figure 10, the model tends to slightly overpredict the burning rate at low crossflow velocities and slightly underpredict it at high velocities.

Theoretical predictions and experimental measurements of erosive burning rates for Formulations 5051, 4685, 4869, 5542T, 5565T and 5555T are presented in Figures 11 through 16. Formulation 5051, which differs from the baseline formulation through use of 200 micron AP oxidizer in place of 20 micron oxidizer, is predicted to be somewhat more sensitive to crossflow than the baseline formulations. Except at low pressure and very high crossflow velocities, agreement between predicted and measured augmentation ratio is fairly good. At low pressure and high crossflow velocity, however, the measured burning rates considerably exceed the predicted values.

As shown in Figure 12, Formulation 4685, which differs from the baseline formulation by replacement of 20 micron oxidizer with 5 micron oxidizer, exhibits considerably less sensitivity to erosion than that baseline formulation, as predicted. Agreement between predicted and observed burning rates appears to be good, except, again, in the low pressure, high crossflow velocity region (less than 2 MPa or 20 atmospheres, greater than 300 to 600 m/sec or 1000 to 2000 ft/sec crossflow velocity). Breakdown of the model presented herein in this pressure-crossflow velocity region is not unexpected since, in this region, the composite propellant begins to behave more like a homogeneous propellant than a heterogeneous propellant, and the model only considers effects of crossflow on the diffusional mixing processes of oxidizer and fuel streams. In order for the model to be useful in low pressure, high crossflow velocity regions, it appears that an additional mechanism beyond that of flame-bending must be involved. With Formulation 4869 (Figure 13), which differs from the baseline formulation through addition of two percent iron oxide catalyst, data and theoretical predictions agree fairly well at high crossflow velocities, but not nearly as well at low crossflow velocities where the predictions of erosive burning rate augmentation are somewhat higher than observed in the experiments. An explanation of this discrepancy has not yet been developed.

With Formulation 5542T (analogous to the baseline formulation but with higher oxidizer/fuel ratio and consequently higher flame temperature and base burning rate, oxidizer size being held constant) the sensitivity to crossflow appears to be somewhat lower than predicted (Figure 14) though the degree of disagreement between data and theory is not large. The data obtained for Formulation 5565T (with approximately the same zero crossflow burning rate-pressure behavior as the baseline formulation, but a considerably higher oxidizer/fuel ratio and flame temperature) presented in Figure 15 are somewhat limited, but indicate reasonable agreement with theory, the formulation being quite sensitive to crossflows. Formulation 5555T (Figure 16), a high burning rate formulation, is predicted to be rather insensitive to crossflows: the data corroborate this prediction.

Next, let us compare results for the various formulations to identify parameters which influence the sensitivity of composite propellants to crossflows. Between Formulations 4525, 5051, and 4685, the only independent variable changed is the oxidizer particle size, composition being held constant. The change of oxidizer size, of course, leads to a change in base (no crossflow) burning rate versus pressure characteristics. Formulation 5051, containing 200 micron diameter AP is the slowest burning of the three formulations, with Formulation 4685 (5 micron AP) being the fastest and Formulation 4525 (20 micron AP) being intermediate. For instance, at 5 MPa (50 atmospheres) the base burning rate of 5051 is 0.47 cm/sec, that of 4525 is 0.68 cm/sec and that of 4685 is 1.15 cm/sec. Examination of Figures 9, 11, and 12 indicates that the sensitivity of burning rate to crossflow increases with increasing particle size (decreasing base burning rate). For example, at a crossflow velocity of 200 m/sec (650 ft/sec) and a pressure of 5 MPa (50 atmospheres), the augmentation ratio for 4685 is about 1.10, that for 4525 is 1.65, and that for 5051 is 2.0.

Comparison of data for 4525 and 4869, two formulations of essentially the same oxidizer/fuel ratio, flame temperature, and oxidizer particle size, with the base burning rate being varied through use of catalyst in 4869, again shows an increase in sensitivity of burning rate to crossflow with a decrease in burning rate. At 5 MPa (50 atmospheres) the base burning rates for 4869 and 4525 are 1.40 cm/sec and 0.68 cm/sec, respectively. At this pressure, with a crossflow velocity of 200 m/sec (650 ft/sec) their r/r_o values are 1.10 and 1.65 respectively, while at 600 m/sec (1950 ft/sec), the r/r_o values are 1.75 and 2.3. Thus base burning rate is seen to affect the erosion sensitivity of composite propellants even at constant oxidizer particle size, erosive effects increasing with decreasing base burning rate.

Formulations 4685 and 4869 have approximately the same base burning rate at 8 MPa (80 atmospheres) with catalyst and oxidizer particle size effects on base burning rate roughly cancelling. Thus comparison of erosion sensitivity of these formulations at this pressure is of interest in that oxidizer particle size is varied (5 micron diameter for 4685, 20 micron diameter for 4869) while base burning rate is held constant. Comparison of data from Figures 12 and 13 indicates that these formulations have roughly the same sensitivity to the lower crossflow velocities tested at 8 MPa (80 atmospheres), with the catalyzed propellant being slightly more sensitive at the higher crossflow velocities tested. Thus it appears that it is the base burning rate rather than the oxidizer particle size per se which dominates the sensitivity of composite propellants to erosive burning, though oxidizer size does have some further residual effect, erosion sensitivity decreasing with decreasing particle size at constant base burning rate.

Comparison of test results for Formulations 4525, 5542T and 5565T permits study of the effect of oxidizer/fuel ratio (and thus flame temperature) on erosion sensitivity, both at constant oxidizer particle size (5542T and 4525) and at constant base burning rate (5565T and 4525). Formulation 5542T differed from 4525 in oxidizer/fuel ratio (77/23 versus 73/27) and consequently flame temperature (2065°K vs. 1667°K). Since the oxidizer particle size was the same for both propellants, the higher oxidizer/fuel ratio for 5542T led to high base burning rate (1.14 cm/sec vs. 0.68 cm/sec at 5 MPa). Study of Figures 9 and 14 reveals that the erosion sensitivity of 5542T is considerably less than that of 4525 over the entire range of crossflow velocities studied (e.g., $r/r_o = 1.10$ for 5542T and 1.65 for 4525 at 200 m/sec, 5 MPa; and $r/r_o = 1.7$ for 5542T and 2.9 for 4525 at 800 m/sec, 5 MPa). Thus we see that changing oxidizer/fuel ratio from very fuel-rich to less fuel-rich, with accompanying increase in flame temperature and burning rate leads to decreased sensitivity to erosive burning. Comparison of results for 5565T and 4525, which differ in oxidizer/fuel ratio but not in base burning rate (oxidizer particle size having been adjusted to compensate for the burning rate change with changing oxidizer/fuel) permits separation of the effects of varying oxidizer/fuel (and thus flame temperature) from the effects of base burning rate. As may be seen by study of Figures 9 and 15, the sensitivity of Formulations 5565T and 4525 to crossflow are nearly the same. For instance, at 200 m/sec (650 ft/sec) crossflow velocity and 5 MPa (50 atmospheres), the augmentation ratios for 5565T and 4525 are 1.50

and 1.65, respectively, while at 800 m/sec (2600 ft/sec) and 3 MPa (30 atmospheres), they are 2.65 and 2.50. Accordingly, we may conclude that oxidizer/fuel ratio (and consequently flame temperature) does not directly affect the erosion sensitivity of the compositions studied to date, but only affects it through its effect on base burning rate.

Formulations 5555T and 5565T had the same composition, differing only in oxidizer particle size, which was adjusted in 5555T to give a very high burning rate. Again, the effect on erosion sensitivity of increased base burning rate can be seen in comparison of Figures 15 and 16. At 5 MPa (50 atmospheres), the base burning rates of 5555T and 5565T are 2.94 and 0.70 cm/sec, respectively. At 200 m/sec (650 ft/sec) crossflow velocities, the respective values of r/r_o are 1.0 and 1.5, while at 700 m/sec (2300 ft/sec), they are 1.2 and 2.4. Thus, once again, erosion sensitivity is seen to decrease with increasing base burning rate.

Summary

An experimental apparatus for measurement of erosive burning rates over a wide range of crossflow velocities, up to Mach 1 has been designed, constructed and checked-out. Erosive burning characteristics of seven formulations, with systematically varied properties, have been measured in this test device and checked against predictions of a first generation composite propellant erosive burning model based upon the bending of columnar diffusion flames. In general, the model appears to give reasonably good agreement with measured erosive burning data, except under conditions where the heterogeneity of the composite propellant is unimportant (low pressure, high crossflow velocity). Here, it appears that an additional mechanism(s) of erosive burning will have to be considered. The data indicate that the base (no crossflow) burning rate versus pressure characteristics of the propellant have a predominant effect on its sensitivity to erosive burning, high burning rate propellants being considerably less sensitive to crossflow than low burning rate formulations, whether the burning rate alterations are produced by oxidizer particle size variation, oxidizer/fuel ratio variations, or use of catalysts. Oxidizer particle size appears to have some effect (but not a great one) beyond its effect on base burning rate, augmentation ratio increasing with increasing particle size. Oxidizer/fuel ratio (and thus flame temperature) appears to affect erosion sensitivity only through its effect on base burning rate.

A review of the literature indicates that the boundary layer profiles in rocket motors may differ significantly from those in typical erosive burning test devices. Comparison of erosive burning calculations using the first generation erosive burning model described in this paper with profiles expected to prevail in the test apparatus versus those estimated to exist in cylindrically perforated motor grains indicate that erosive burning may be considerably less for a given mainstream crossflow velocity in such a motor than in a typical erosive burning testing apparatus, indicating a strong need for further study of boundary layer profiles in the near-wall region in rocket motor grain ports.

Nomenclature

A_3, A_4, A_5	empirical constants relating no-crossflow burning rate to pressure (Equation 3), obtained by regression analysis
d_p	oxidizer particle diameter
D	flow channel hydraulic diameter
L_I	oxidizer monopropellant reaction kinetic distance (Fig. 1)
L_{Diff}	oxidizer-fuel gas mixing distance (Fig. 1)
L_{Kin}	oxidizer-fuel reaction (kinetic) distance (Fig. 1)
M	crossflow mainstream Mach Number
$\dot{m}$	mass flux, measured in direction of resultant of crossflow and propellant transpiration flow
$\dot{m}_{burn}$	propellant burning mass flux
P	pressure
$\dot{q}$	heat feed-back flux from gas to propellant surface
r	propellant burning rate
r_o	propellant burning rate with no crossflow
T_{AP}	ammonium perchlorate monopropellant flame temperature
T_f	final flame temperature
T_s	surface temperature
$\bar{u}$	mean crossflow velocity
u^+	dimensionless crossflow velocity
u_y	crossflow velocity at distance y from surface
y^+	dimensionless distance from propellant surface
θ	flow angle (Figures 1, 2)
ρ_p	propellant density

References

1. King, M., "Effects of Crossflow on Solid Propellant Combustion: Interior Ballistic Design Implications," 1976 JANNAF Propulsion Meeting, Atlanta, Georgia, December 1976, CPIA Publ. 280, Vol. V, p. 342.

2. Viles, J.M., "Prediction of Rocket-Motor Chamber Pressures Using Measured Erosive-Burning Rates," Technical Report S-275 (Contract DAAH01-70-C-0152), Rohm and Haas Co., Huntsville, Alabama 35807, October 1970.

3. Saderholm, C.A., "A Characterization of Erosive Burning for Composite H-Series Propellants," AIAA Solid Propellant Rocket Conference, Palo Alto, California, January 29, 1964.

4. Kreidler, J.W., "Erosive Burning: New Experimental Techniques and Methods of Analysis," AIAA Solid Propellant Rocket Conference, Palo Alto, California, January 29, 1964.

5. Schultz, R., Green, L., and Penner, S.S., "Studies of the Decomposition Mechanism, Erosive Burning, Sonance and Resonance for Solid Composite Propellants," Combustion and Propulsion, 3rd AGARD Colloquium, Pergamon Press, N.Y., 1958.

6. Green, L., "Erosive Burning of Some Composite Solid Propellants," Jet Propulsion, 24, 9, 1954.

7. Peretz, A., "Experimental Investigation of the Erosive Burning of Solid Propellant Grains with Variable Port Area," AIAA Journal, 6, 910, 1968.

8. Marklund, T., and Lake, A., "Experimental Investigation of Propellant Erosion," ARS Journal, 30 173, 1960.

9. Dickinson, L.A., Jackson, F., and Odgers, A.L., "Erosive Burning of Polyurethane Propellants in Rocket Engines," Eighth Symposium (International) on Combustion, 754, Williams and Wilkins. Baltimore, 1962.

10. Zucrow, M.J., Osborn, J.R., and Murphy, J.M., "An Experimental Investigation of the Erosive Burning Characteristics of a Nonhomogeneous Solid Propellant," AIAA Journal, 3, 523, 1965.

11. Vilyunov, V.N., Dvoryashin, A.A., Margolin, A.D. Ordzhonikidze, S.K., and Pokhil, P.R., "Burning of Ballistite Type H in Sonic Flow," Fizika Goreniya i Vzryva, 8, 4, 501-5, October-December 1972.

12. King, M., "Erosive Burning of Composite Propellants," 13th JANNAF Combustion Meeting, Monterey, California, September 1976, CPIA Publ. 281, Vol. II, p. 407.

13. King, M., "A Model of the Erosive Burning of Composite Propellants," AIAA/SAE 13th Propulsion Conference, Orlando, Florida, July, 1977, AIAA Paper 77-930.

14. Lengelle, G., "Model Describing the Erosive Combustion and Velocity Response of Composite Propellants," AIAA Journal, 13, 3, 315-322, March 1975.

15. Beddini, R.A., Varma, A.K., and Fishburn, E.S., "A Preliminary Investigation of Velocity-Coupled Erosive Burning," 13th JANNAF Combustion Meeting, Monterey, California, September, 1976, CPIA Publication 281, Vol. II, p. 385

16. Beddini, R., and Fishburne, E., "Analysis of the Combustion-Turbulence Interaction Effects on Solid Propellant Erosive Burning," AIAA Paper 77-931, AIAA 13th Propulsion Conference, Orlando, Florida, July, 1977.

17. Beddini, R.A., A Reacting Turbulent Boundary Layer Approach to Solid Propellant Erosive Burning, AFOSR Scientific Report, AFOSR-TR-77-1310, November, 1977.

18. Razdan, M., and Kuo, K., Erosive Burning Studies of Composite Solid Propellants by the Reacting Turbulent Boundary-Layer Approach, AFOSR Scientific Report, AFOSR-TR-78-0035, November 1977.

19. Condon, J., and Osborn, J.R., The Effect of Oxidizer Particle Size Distribution on the Steady and Nonsteady Combustion of Composite Propellants, Final Report, Jet Propulsion Center, Purdue University, Report AFRPL-TR-78-17, April 1978.

20. Beckstead, M.W., Derr, R.L., and Price, C.F., "The Combustion of Solid Monopropellants and Composite Propellants," Thirteenth International Symposium on Combustion, The Combustion Institute, Pittsburgh, Pennsylvania, 1971, pp. 1047-1056. Also, "Combustion Tailoring Criteria for Solid Propellants," Lockheed Propulsion Company Report 835F (AFRPL-TR-69-190), May, 1969.

21. King, M.K., "Model for Steady State Combustion of Unimodal Composite Solid Propellants," AIAA 16th Aerospace Sciences Meeting, Huntsville, Alabama, AIAA Paper No. 78-216, Jan. 1978.

22. Mickley, H.S., and Davis, R.S., "Momentum Transfer for Flow Over a Flat Plate with Blowing," NACA Technical Note 4017, November 1975.

23. Yamada, K., Goto, M., and Ishikawa, N., "Simulative Study on the Erosive Burning of Solid Rocket Motors, AIAA Journal, 14, 9, p. 1170, September, 1976.

24. Dunlap, R., Willoughby, P.G., and Hermsen, R.W., "Flowfield in the Combustion Chamber of a Solid Propellant Rocket Motor," AIAA Journal, 12, 10, p. 1440, October, 1974.

25. Lenoir, J.M., and Robillard, G., "A Mathematical Method to Predict the Effects of Erosive Burning in Solid-Propellant Rockets," Sixth Symposium (International) on Combustion, 663, Reinhold Publishing Corp., New York, 1957.

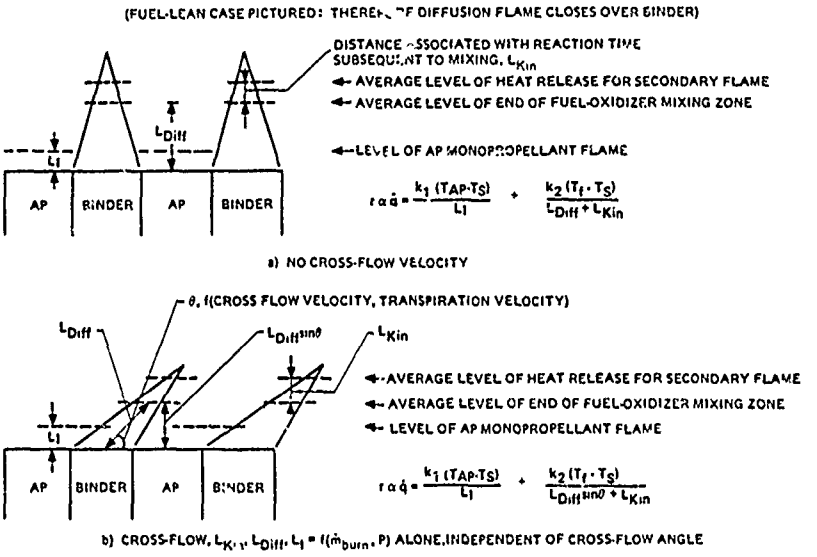

Figure 1. Schematic of Geometrical Model of Erosive Burning (Two-Flame Model).

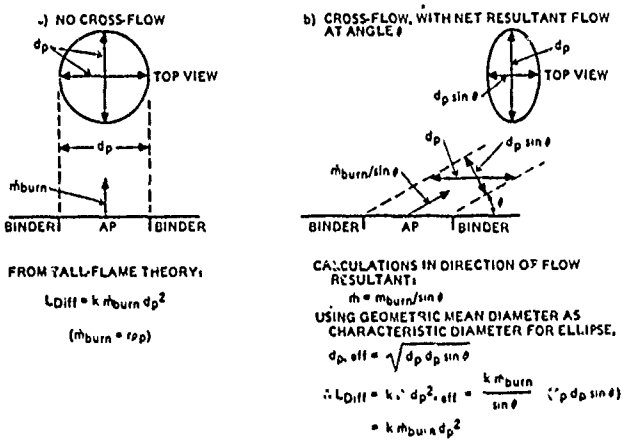

Figure 2. Approximate Calculations of Dependency of Diffusion Distance Measured in the Direction of Resultant Flow (L_{Diff}) on Flow Angle, At Constant Propellant Burning Rate ($\dot{m}_{burn}$).

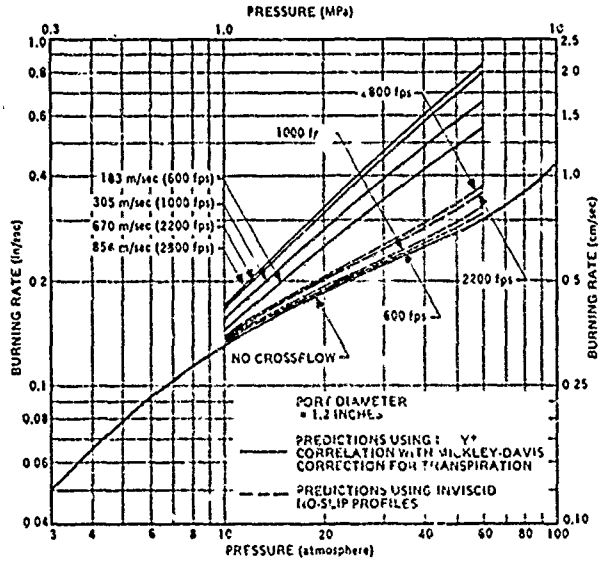

Figure 3. Erosive Burning Rate Predictions with the First Generation Model Using Mickley-Davis Boundary Layer Profiles and Using Inviscid No-Slip Wall Boundary Layer Profiles. Formulation 4525 (73/27 AP/HTPB, 20 micron Diameter AP).

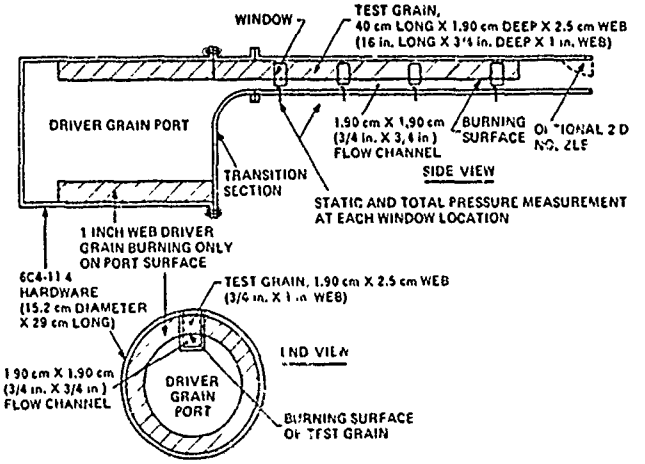

Figure 4. Sketch of Test Hardware.

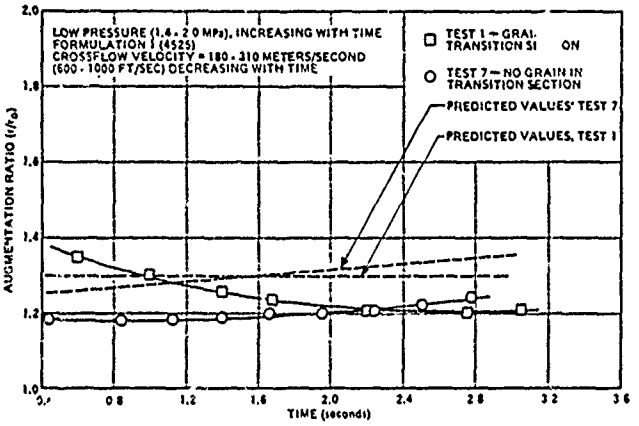

Figure 5. Comparison of Erosive Burning with and Without Test Grain Extending Thru Transition Section to Mate with Driver Grain - Low Pressure.

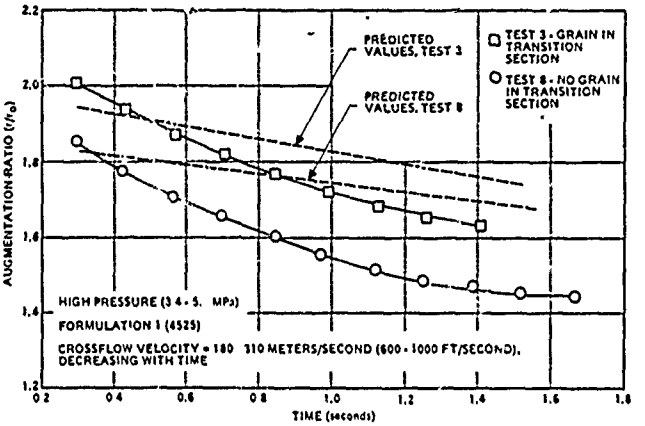

Figure 6. Comparison of Erosive Burning with and Without Test Grain Extending Thru Transition Section to Mate with Driver Grain - High Pressure.

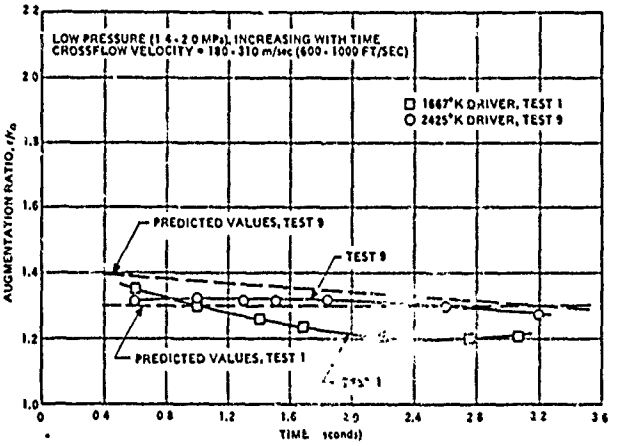

Figure 7. Comparison of Erosive Burning of Formulation 1 (4525) with 1667°K Driver Grain and 2425° Driver Grain - Low Pressure.

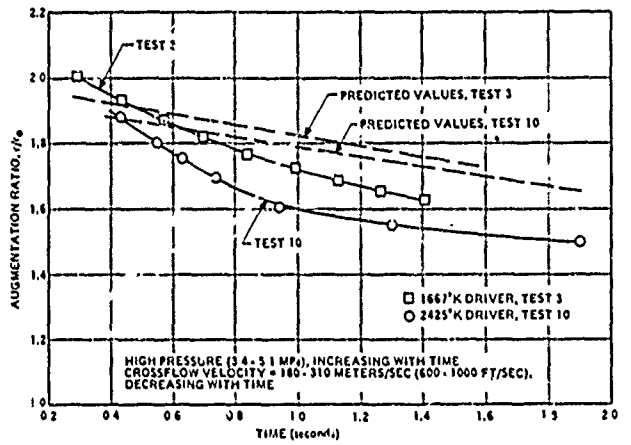

Figure 8. Comparison of Erosive Burning of Formulation 1 (4525) with 1667°K Driver Grain and 2425° K Driver Grain - High Pressure.

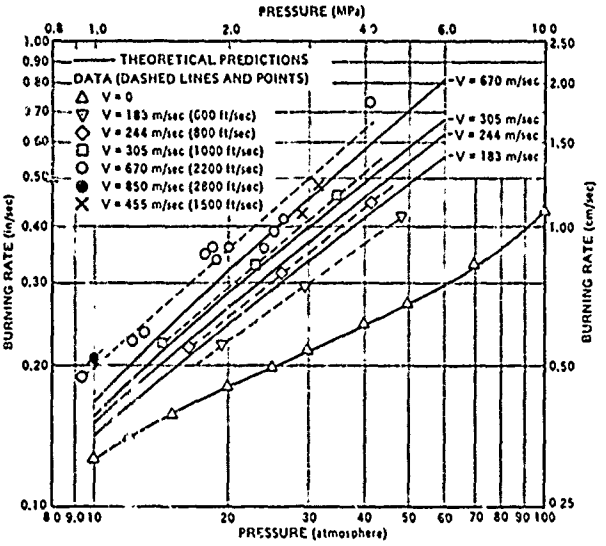

Figure 9. Theoretical and Experimental Burn Rate - Pressure Relationships for Various Crossflow Velocities for Formulation 4525 (1667°K Formulation, 73/27 AP/HTPB, 20 Micron AP).

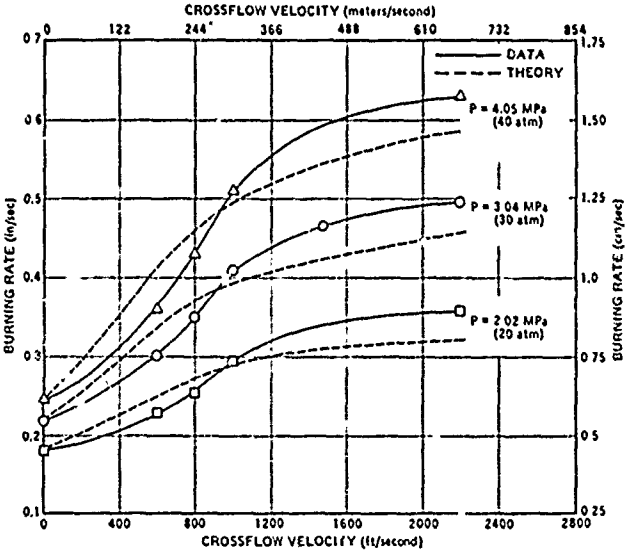

Figure 10. Burning Rate Versus Crossflow Velocity Data and Predictions for Formulation 4525 (73/27 AP/HTPB, 20 Micron AP).

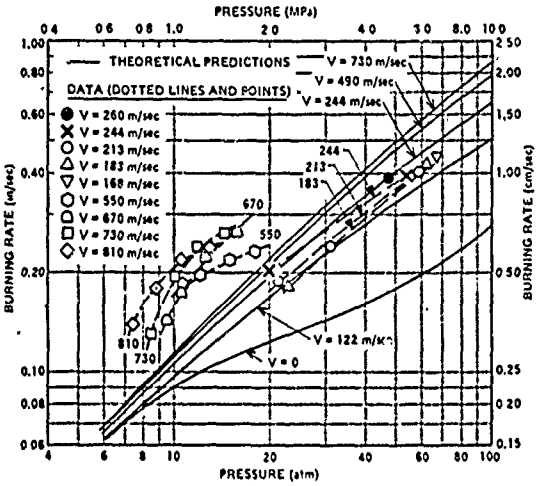

Figure 11. Theoretical and Experimental Burn Rate - Pressure Relationships for Various Crossflow Velocities for Formulation 5051 (1667°K Formulation, 73/27 AP/HTPB, 200 Micron AP).

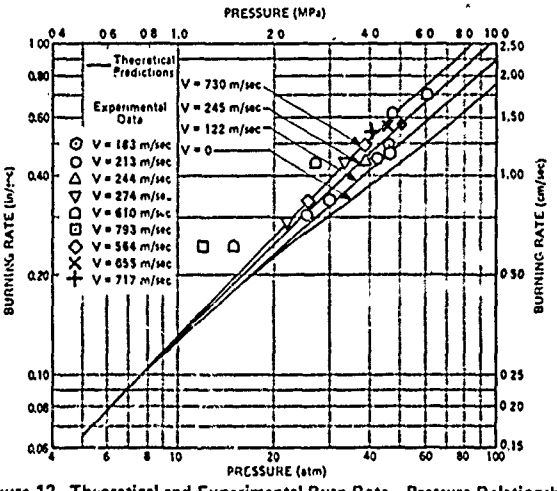

Figure 12. Theoretical and Experimental Burn Rate - Pressure Relationships for Various Crossflow Velocities for Formulation 4685 (1667°K Formulation, 73/27 AP/HTPB, 5 Micron AP).

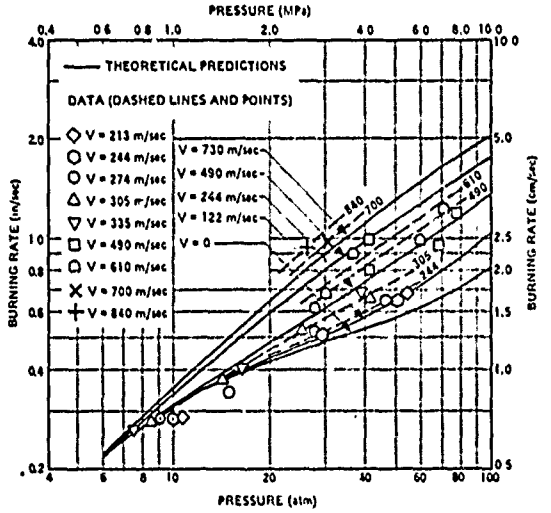

Figure 13. Theoretical and Experimental Burn Rate - Pressure Relationships for Various Crossflow Velocities for Formulation 4869 (1667°K Formulation, 72/26/2 AP/HTPB/Fe_2O_3, 20 Micron AP).

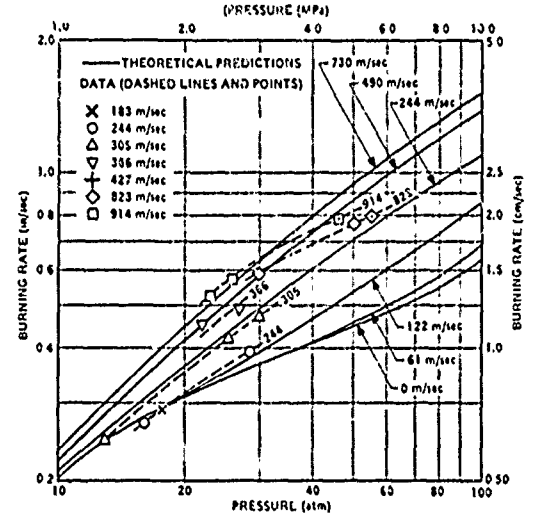

Figure 14. Theoretical and Experimental Burn Rate - Pressure Relationships for Various Crossflow Velocities for Formulation 5542T (2065°K Formulation, 77/23 AP/HTPB, 20 Micron AP).

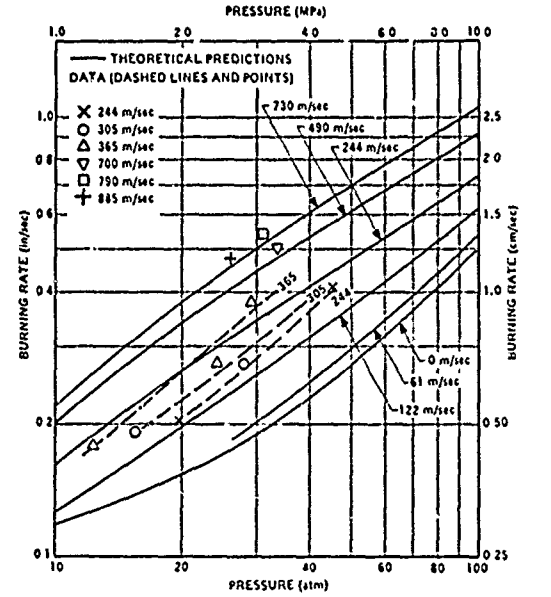

Figure 15. Theoretical and Experimental Burn Rate - Pressure Relationships for Various Crossflow Velocities for Formulation 5565T (2575°K Formulation, 82/18 AP/HTPB, Bimodal With Sizes Chosen to Match 4525 Burning Rate).

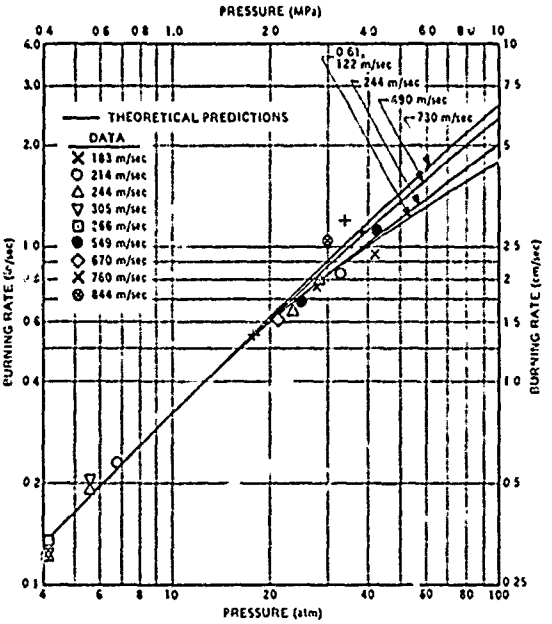

Figure 16. Theoretical and Experimental Burn Rate - Pressure Relationships for Various Crossflow Velocities for Formulation 5555T (2575°K Formulation, 82/18 AP/HTPB, High Burn Rate).

UNCLASSIFIED

SECURITY CLASSIFICATION OF THIS PAGE (When Data Entered)

REPORT DOCUMENTATION PAGE	READ INSTRUCTIONS BEFORE COMPLETING FORM
1. REPORT NUMBER (19) (18) AFOSR TR—79—0435	2. GOVT ACCESSION NO. / 3. RECIPIENT'S CATALOG NUMBER
4. TITLE (and Subtitle) (6) EROSIVE BURNING OF COMPOSITE SOLID PROPELLANTS: EXPERIMENTAL AND MODELING STUDIES,	5. TYPE OF REPORT & PERIOD COVERED Interim
	6. PERFORMING ORG. REPORT NUMBER
7. AUTHOR(s) (10) Merrill K. King	8. CONTRACT OR GRANT NUMBER(s) (15) F49620-78-C-0016, F44620-76-C-0073
9. PERFORMING ORGANIZATION NAME AND ADDRESS Atlantic Research Corporation 5390 Cherokee Avenue Alexandria, Virginia 22314	10. PROGRAM ELEMENT, PROJECT, TASK AREA & WORK UNIT NUMBERS (16) 2308 (17) A1 61102F
11. CONTROLLING OFFICE NAME AND ADDRESS Air Force Office of Scientific Research/NA Building 410 Bolling AFB, DC 20332	12. REPORT DATE (11) August 1978 13. NUMBER OF PAGES (12) 140.
14. MONITORING AGENCY NAME & ADDRESS (if different from Controlling Office)	15. SECURITY CLASS. (of this report) UNCLASSIFIED
	15a. DECLASSIFICATION/DOWNGRADING SCHEDULE

16. DISTRIBUTION STATEMENT (of this Report)

Approved for public release; distribution unlimited

17. DISTRIBUTION STATEMENT (of the abstract entered in Block 20, if different from Report)

18. SUPPLEMENTARY NOTES

19. KEY WORDS (Continue on reverse side if necessary and identify by block number)

Erosive burning
Composite Propellants
Propellant Combustion Modeling
Nozzleless Rocket Motors

20. ABSTRACT (Continue on reverse side if necessary and identify by block number)

An experimental apparatus designed for measurement of erosive burning rates at crossflow velocities up to Mach 1 has been used to determine the erosive burning characteristics of seven propellant formulations with systematically varied properties. A composite propellant erosive burning model based on the bending of columnar diffusion flames gives reasonably good agreement with the measured erosive burning data over a wide range of conditions, breaking down onl in regions where the fuel-oxidizer gas stream mixing does not control burning

(over)

rate. Propellant base (no-crossflow) burning rate is found to have a predominant effect on sensitivity to crossflow (higher-burning-rate formulations being considerably less sensitive) whether the base burning rate differences are produced by oxidizer particle size variation, oxidizer/fuel ratio variation, or use of catalysts. Comparison of erosive burning predictions using the erosive burning model described herein with flow profiles expected to prevail in the test apparatus to predictions using profiles believed to exist in cylindrically-perforated motor grains indicate that erosive burning may be considerably less for a given mainstream crossflow velocity in such a motor than in the typical erosive burning test apparatus, a result quite important to extrapolation of test apparatus erosive burning data to actual motor conditions.